

Cubic crystal protein inclusions in the neodermis of the pancreatic fluke, *Eurytrema pancreaticum*, and *Eurytrema coelomaticum*

Tsukasa Sakamoto · Tetsuo Oikawa

Received: 15 March 2007 / Revised: 23 June 2007 / Accepted: 27 June 2007 / Published online: 27 July 2007
© Springer-Verlag 2007

Abstract Light microscopy of *Eurytrema pancreaticum* and *Eurytrema coelomaticum* collected from cattle in Japan, China, Thailand, and Brazil showed many cubic crystal inclusions in the neodermis (tegument) of all flukes. The crystal inclusions were histochemically positive for protein. Scanning electron microscopy showed many cubic protrusions containing cubic crystal protein inclusions on the surface of the neodermis. Transmission electron microscopy showed that cubic crystal protein inclusions appeared in the perikarya of subtegumental parts, passed through the cytoplasmic bridge, moved into the syncytial neodermal cytoplasm, and then protruded from, and finally separated from, the neodermal cytoplasm. Cubic crystal protein inclusions were hexahedral with each side 2–18 μm long. High-resolution microscopy of ultrathin sections of crystal inclusions showed a lattice fringe at spacings of about 0.52 nm by using a filtering processing. Diffractograms were obtained by Fourier transform of the images. The lattice structure of the crystal protein inclusions was shown by inverse Fourier transform, indicating that the cubic

crystal protein inclusions were single crystals. Sodium dodecyl sulfate–polyacrylamide gel electrophoresis estimated the molecular weight of protein in the cubic crystal inclusion as 36.6 kDa. Energy-dispersive X-ray spectroscopy proved that the cubic crystal protein inclusions were composed of protein and sulfur.

Introduction

Nine species have been reported from the genus *Eurytrema* in the family Dicrocoeliidae (Yamaguti 1958), of which *Eurytrema pancreaticum* and *Eurytrema coelomaticum* are common flukes in pancreatic and bile ducts of ruminants. Taxonomic confusion used to be between the two species, but comparative studies of the two species showed morphological differences (Yamaguti 1958, 1971; Tang and Tang 1977; Sakamoto et al. 1980; Chinone et al. 1984), and their karyotypes are clearly distinct (Moriyama 1982).

E. pancreaticum and *E. coelomaticum* are highly prevalent in China (Tang and Tang 1977), Japan (Sakamoto et al. 1980), and Thailand (Khawsuk et al. 2002), and *E. coelomaticum* is endemic in Brazil (Ilha et al. 2005). Numerous cubic crystal inclusions, reported as “cubic corpuscles” (Sakamoto et al. 1985), are in the neodermis (tegument) of *E. coelomaticum* shown by using light and electron microscopy. From the viewpoint of the site of occurrence, shape, and ingredients of the cubic crystal inclusions, however, the name of “cubic corpuscle” is renamed as “cubic crystal protein inclusion” in this paper. We believe cubic crystal protein inclusions in *Eurytrema* spp. have not been described. Therefore, this study aimed to clarify the crystal structure, development, and biochemical properties of the cubic protein crystal inclusions in the neodermis of *E. pancreaticum* and *E. coelomaticum*.

T. Sakamoto
School of Veterinary Medicine, Faculty of Agriculture,
Iwate University,
Ueda 3-chome 18-8, Morioka,
Iwate 020-8550, Japan

T. Oikawa
Applied Microscope Group, Application and Research Center,
Electron Optics, JEO,
1-2, Musashino 3-chome Akishima,
Tokyo, Japan

T. Sakamoto (✉)
Sumikawa 5-jyo, 11-chome, Minami-ku,
Sapporo 005-0005, Japan
e-mail: tsukasakamoto@ybb.ne.jp

Materials and methods

Parasites

E. pancreaticum and *E. coelomaticum* were collected from the pancreatic and bile ducts of cattle at abattoirs in Japan, China, Thailand, and Brazil. Some flukes were flattened between two slides and were fixed in 70% ethanol. The specimens were stained with carmine or hematoxylin and were morphologically examined to identify the species. Flukes collected from Shimane Prefecture, Japan, were *E. pancreaticum* only, flukes from the Kagoshima Prefecture, Japan, and from Fujian Province of China and South Thailand were *E. pancreaticum* and *E. coelomaticum*, and all flukes from Parana State, Brazil, were *E. coelomaticum* only.

Cubic crystal protein inclusions

The flukes were agitated for 3 min with a bar magnet in a beaker containing 100 ml of phosphate buffer solution (PBS) on a magnetic stirrer. Cubic crystal protein inclusions separated from the neodermis of the flukes were collected by centrifugation at 3,000 rpm for 5 min. Cellular elements from the parasite tissue were separated from the cubic crystal protein inclusions by density gradient centrifugation. The purified crystal protein inclusions were used for morphological and analytical observation.

Histological and histochemical examination

The flukes were fixed in either acetone, Carnoy fixative, or 10% neutral formalin and were dehydrated in an ethanol series and then were embedded in paraffin. Sections were stained with either hematoxylin–eosin (HE) or Azan stain for histological examination. Histochemical examination was by using mercuric bromophenol blue staining for protein and peptide (Mazia et al. 1953), periodic acid–Schiff (PAS) reaction with or without salivary or diastase treatment for polysaccharide and glycogen, toluidine blue staining for acidic mucopolysaccharides and hyaluronic acid, and methylgreen–pyronin staining for deoxyribonucleic acid (DNA) and ribonucleic acid (RNA), Sudan black B or Sudan III staining for lipid and neutral fat, and van Kossa's test for calcium phosphate and calcium carbonate.

Scanning electron microscopy

About 40 flukes of each species were fixed in 2.5% cold glutaraldehyde in PBS at pH 7.4 for 1 h. Half the number of flukes were then postfixed in 1% osmium tetroxide in PBS at pH 7.4 for 2 h and were dehydrated in an ethanol series. The dehydrated specimens were then washed with three

changes of pure isoamylacetate and were dried by using the critical point method with liquid CO₂. The dried flukes were mounted on a block were sputter coated with gold and were observed at an accelerating voltage of 15 kV using scanning electron microscopy (SEM).

Transmission electron microscopy

The remaining specimens were fixed in 2.5% glutaraldehyde, were postfixed in 1% osmium-tetroxide, were dehydrated in an ethanol series, were embedded in Epon 812 and were sectioned. Ultrathin sections were mounted on nickel or copper grids, were stained with saturated uranyl and lead citrate and were observed by using transmission electron microscopy (TEM).

High-resolution electron microscopy

Ultrathin sections of cubic crystal protein inclusions were examined by using the high-resolution electron microscope JEM-2010/-PIXSYSTEM. Images of the high-resolution electron microscopy (HREM) were processed to remove interference by electrons. Diffractograms were obtained by the fast Fourier transform (FFT) of the images of HREM. The data of diffractograms were processed by inverse Fourier transform.

Biochemical observation of cubic crystal protein inclusions

Purified crystal protein inclusions separated from the neodermis of the flukes were recentrifuged at 12,000 rpm for 5 min, and the sediment was dissolved in 20 µl of sample buffer solution (125 mM Tris–HCl at pH 6.8, 4% sodium dodecyl sulfate [SDS], 30% glycerol, 5% 2-mercaptoethanol). The solution was heated for 5 min in a hot water bath. SDS–polyacrylamide gel electrophoresis (SDS–PAGE) of the sample was done by using a 2–2.5% gradient gel plate with a molecular weight marker (DAIICH III, Daiichi Pure Chemicals, Tokyo, Japan; Laemmli 1970). Then, the separated bands were stained with Coomassie brilliant blue (CBB) or by using a silver-staining kit (BioRad). The molecular weight of the protein composing the cubic crystal protein inclusions was estimated from the standard curve.

Analysis was performed by using an energy-dispersive X-ray spectroscopy.

Twenty flukes of each species fixed in 2.5% glutaraldehyde only were embedded in Epon 812 and were sectioned. Ultrathin sections of the specimens were mounted on copper grids and were analyzed by using TEM combined with an energy-dispersive X-ray spectroscopy (EDS). Cubic crystal protein inclusions released from the neodermis of the flukes were mounted on an aluminum block and were analyzed by using an SEM combined with an EDS.

Results

Morphology

Morphological features differentiated *E. pancreaticum* and *E. coelomaticum*. The body size of *E. pancreaticum* (12.5–18.0×5.5–6.0 mm) was markedly larger than that of *E. coelomaticum* (5.0–8.2×1.2–4.7 mm). The oral sucker of *E. pancreaticum* (0.9–1.7 mm diameter) was larger than its ventral sucker (0.8–0.9 mm), but the oral sucker of *E. coelomaticum* (0.8–0.9 mm diameter) was equal in size or smaller than its ventral sucker (0.83–0.85 mm). *E. pancreaticum* and *E. coelomaticum* egg sizes were 0.046–0.076×0.028–0.040 and 0.042–0.052×0.023–0.038 mm, respectively.

Many hexahedral crystalloids (cubic crystal protein inclusions) were scattered on the neodermal surface of all specimens stained with carmine or hematoxylin, indicating that they occurred constantly in both species regardless of the country of origin of the cattle examined. Many free cubic crystal protein inclusions were also in the pancreatic duct. The cubic crystal protein inclusions free from the parasite tissue were regular hexahedral of sides 2–18 μm.

Histology and histochemistry

E. pancreaticum and *E. coelomaticum* showed no fundamental difference in histology. The neodermis (tegument) of both flukes was histologically differentiated as an outer syncytial anuclear neodermal layer and syncytial nucleated subtegumental parts (perikarya) of the neodermis. Cubic crystal protein inclusions were in the neodermis and in the subtegumental parts in the parenchyma. The crystal protein inclusions were regular hexahedral. Cubic crystal protein inclusions in flukes fixed in 10% neutral formalin were poorly eosinophilic with HE, but crystal inclusions in flukes fixed in Carnoy's solution were stained deep red with HE (Fig. 1). Cubic crystal protein inclusions were stained deep scarlet with Azan stain and were strongly positive for protein with mercuric bromophenol blue staining. However, they were negative in a PAS reaction, were negative for DNA and RNA with methylgreen–pyronin staining, showed no metachromasia with toluidine blue staining, were scarcely stained with Sudan III and Sudan black, and were negative in van Kossa's test.

Scanning electron microscopy

Many cubic crystal protein inclusions covered with neodermal cytoplasm protruded beyond the neodermis of both species (Figs. 2, 3, and 4). Pits caused by separation of the cubic crystal protein inclusions were often on the neo-

dermal surface (Fig. 5). Crystal protein inclusions released from the neodermis of the flukes were regular cubes (Fig. 6, inset) as seen by light microscopy (Fig. 6). Cubic crystal protein inclusions were not on the genital pore (Fig. 2) and oral and ventral suckers (Fig. 5).

Transmission electron microscopy

The neodermis of the flukes was essentially differentiated as an outer anuclear syncytial neodermal cytoplasm (syncytial distal cytoplasm) and a nucleated subtegumental cytoplasm (perikarya of the subtegumental cytoplasm) in the parenchyma. The outer anuclear syncytial neodermal cytoplasm was connected by cytoplasmic bridges to the underlying perinuclear cytoplasm of the nucleated subtegumental cytoplasm. In the neodermis of adult flukes, the outer anuclear neodermal layer, in the sense of the word by light microscopy, corresponds to a distal syncytial neodermal cytoplasm of subtegumental cells as seen by TEM. In this study, the outer surface of the neodermis (tegument) of both species was covered with an outer neodermal cytoplasm having microvilli. Many vesicles and tubules and some mitochondria were in the neodermal cytoplasm. Small cubic crystal protein inclusions were sometimes near the Golgi complex in the perikarya of subtegument. Comparatively small cubic crystal protein inclusions were in the perikarya of the subtegument (Fig. 7) and in the cytoplasmic bridges (Fig. 8) linking the distal neodermal cytoplasm and subtegumental portions. The cubic crystal protein inclusions were larger in the neodermal cytoplasm and protruded from the cytoplasm surface (Fig. 9).

High-resolution electron microscopy

HREM of ultrathin sections of cubic crystal protein inclusions showed lattice fringes. A lattice-like structure was shown by filter processing lattice fringes of the cubic crystal protein inclusions (Fig. 10). The spacings of the lattice-like structure were about 0.52 nm (range 0.42–0.63). Diffractograms were obtained by FFT of the image. The patterns were strong spots surrounded by many weak spots. Lattice structures were shown by inverse Fourier transform of the diffractograms, but they were slanted (Fig. 10, inset).

Biochemical analysis of cubic crystal protein inclusions

SDS-PAGE was done to estimate the molecular weight of the protein in the cubic crystal protein inclusions. Figure 11 shows the separated bands. The molecular weight of the protein composing the cubic crystal inclusions was estimated as 36.6 kDa.

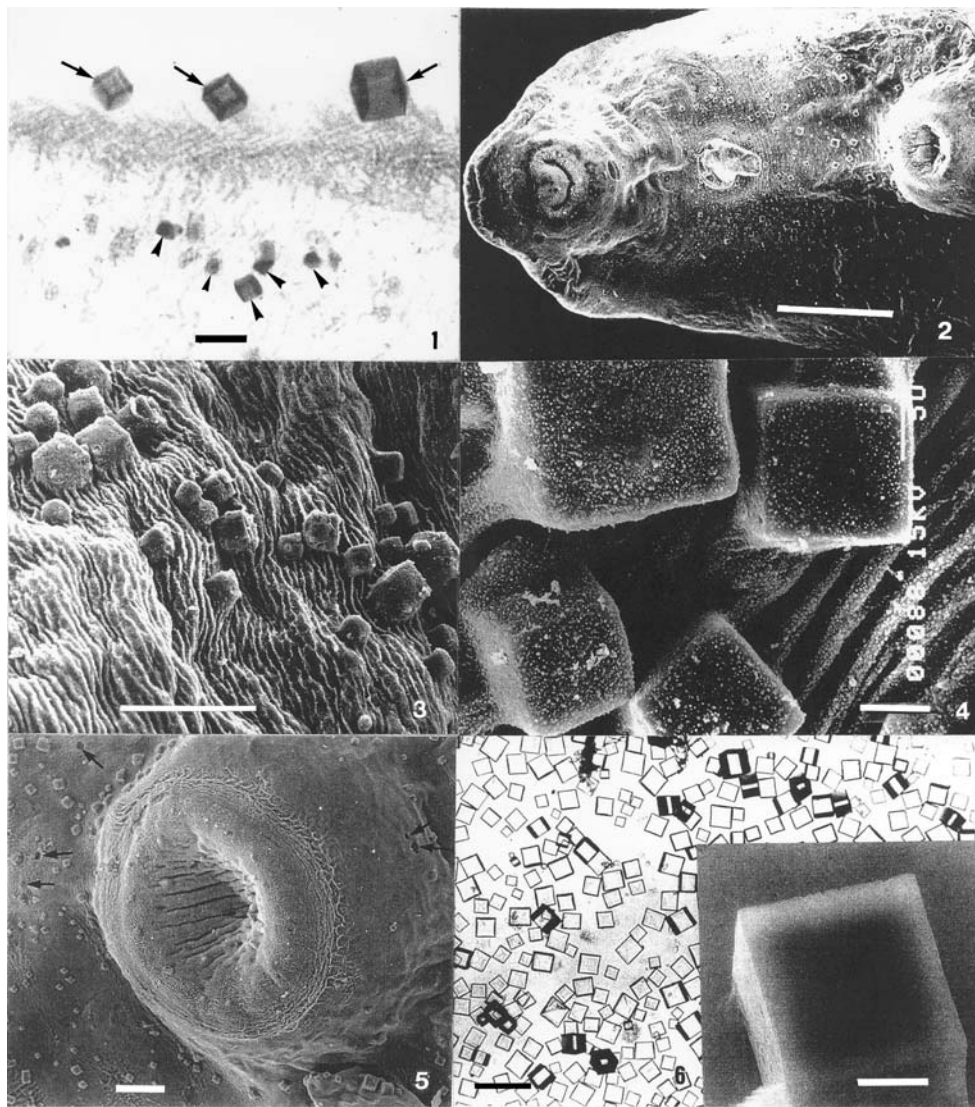


Fig. 1 Light micrograph of cubic crystal protein inclusions of an adult *E. pancreaticum*. Big cubic crystal protein inclusions (*arrows*) are in the outer anuclear neodermal layer, and small inclusions (*arrowheads*) are in the syncytial nucleated subtegumental portions of the neodermis in the parenchyma (HE stain). *Bar*=20 μ m

Fig. 2 Anterior part of an adult *E. coelomaticum*. Many cubic crystal protein inclusions are on the surface of the neodermis. SEM, *bar*=250 μ m

Fig. 3 Cubic crystal protein inclusions on the neodermis of an adult *E. pancreaticum*. The many crystal protein inclusions are covered with the neodermal cytoplasm. SEM, *bar*=50 μ m

Fig. 4 Cubic crystal protein inclusions on the neodermal cytoplasm of an adult *E. coelomaticum*. The crystal protein inclusions are covered with a neodermal cytoplasm having microvilli. SEM, *bar*=5 μ m

Fig. 5 Cubic crystal protein inclusions on the neodermis surrounding the ventral sucker of an adult *E. pancreaticum*. Pits (*arrows*) caused by the separation of cubic crystal protein inclusions are on the neodermis. SEM, *bar*=50 μ m

Fig. 6 Light micrograph of purified cubic crystal protein inclusions released from the neodermis of adult flukes of *E. coelomaticum*. *Bar*=50 μ m. *Inset*: Scanning electron micrograph of a cubic crystal protein inclusion separated from the neodermal cytoplasm of an adult *E. coelomaticum*. *Bar*=10 μ m

Energy-dispersive X-ray spectroscope

Ultrathin sections of the specimens mounted on a copper grid were observed by using an analytical TEM combined with an EDS. A spike corresponding to sulfur was detected

next to a spike of copper derived from the grid. Purified cubic crystal protein inclusions mounted on an aluminum block were observed by using an analytical SEM combined with an EDS. A spike corresponding to sulfur and a spike of aluminum derived from the blocks were detected (Fig. 12).

Fig. 7 A cubic crystal protein inclusion in the perikaryon of a subtegumental cell in the parenchyma of an adult *Eurytrema pancreaticum*. TEM, bar=5 μm

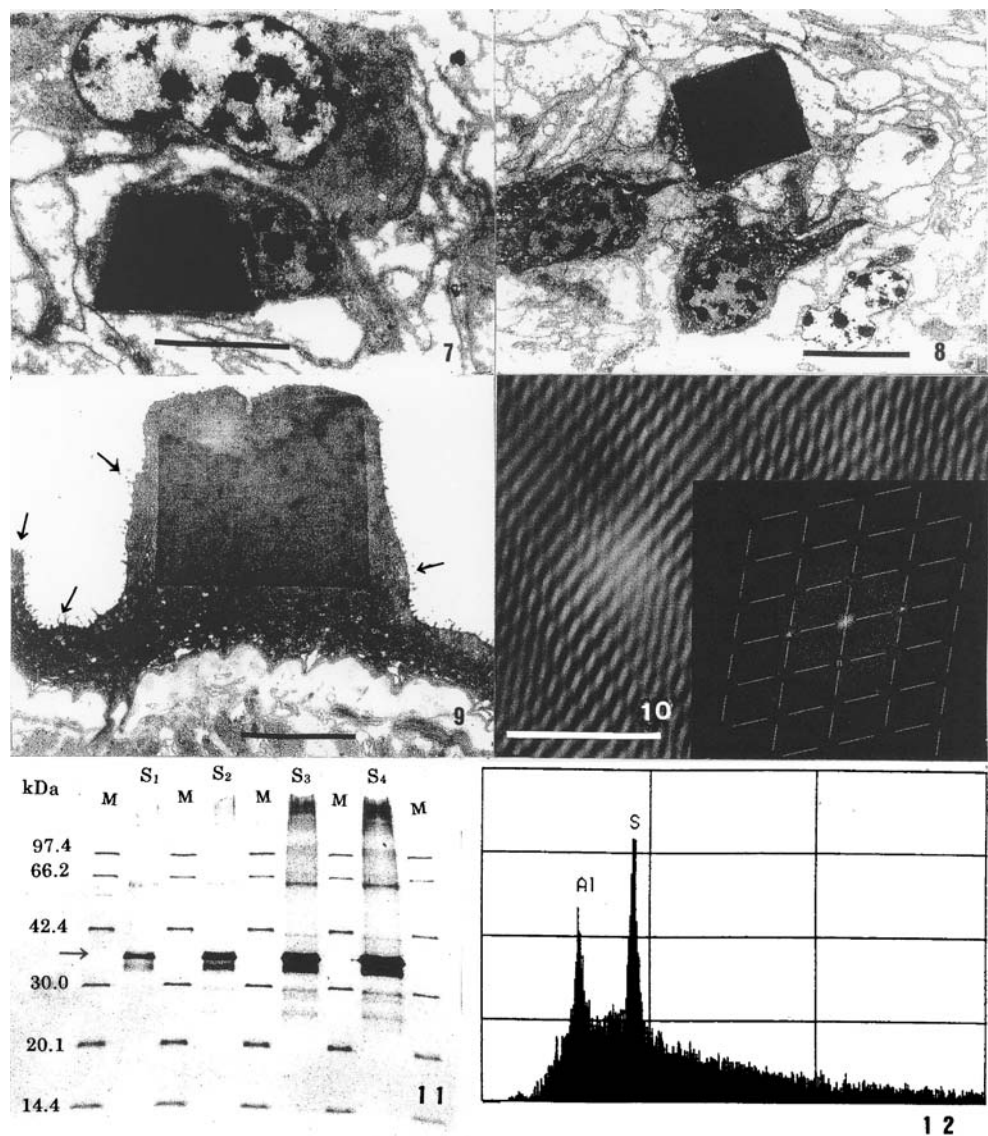
Fig. 8 A cubic crystal protein inclusion in the cytoplasmic bridge of a subtegumental cell. TEM, bar=5 μm

Fig. 9 A cubic crystal protein inclusion covered with neodermal cytoplasm having microvilli (arrows) on its surface. TEM, bar=5 μm

Fig. 10 Lattice fringe of a cubic crystal protein inclusion shown by filtering in a high-power micrograph. Bar=5 nm. Inset: Lattice structure shown by inverse Fourier transformation of the diffractogram obtained by FFT process

Fig. 11 A band (arrow) of protein from cubic crystal protein inclusions on the gel plate treated by SDS-PAGE. Sample solution was applied at 1, 2, 4, and 8 μl to wells S₁₋₄, respectively. Molecular weight markers are indicated in kDa on the left side (silver stain)

Fig. 12 X-ray microanalytical image of a cubic crystal protein inclusion. Spikes for sulfur (S) and aluminum (Al) are shown, but Al originated from the aluminum block



Discussion

Cubic crystal protein inclusions were in the neodermis of all specimens, indicating that they occurred constantly in both species regardless of the country of origin of the cattle. Based on the histological and electron microscopical findings in this study, the following process can be inferred: cubic crystal protein inclusions may first appear in the Golgi complex of the subtegumental parts of the neodermis, then pass through the cytoplasmic bridges, move into the neodermal cytoplasm, protrude from the neodermal surface as their size increases, and finally separate from the neodermal cytoplasm by rupturing the neodermal membrane. Lattice-like structures having spacings of average 0.52 nm were shown by filtering the lattice fringe obtained by HREM of the cubic crystal protein inclusions. A diffractogram was obtained by Fourier transform of the lattice image, and lattice structures of the crystal protein

inclusions were shown by inverse Fourier transform of the diffractogram. These results support the view that cubic crystal protein inclusions are a single crystal. Crystal protein inclusions released from the neodermis of the fluke were recognized as regular cubes by using light microscopy (Figs. 1, 6) and SEM (Fig. 6, inset). The high-magnification observations of crystal protein inclusions in this study showed that the lattice structures were slanted (Fig. 10, inset), and so, a lattice constant could not be calculated. The lattice of the crystals has a slanting lattice structure because of the procedure of sectioning, fixing, or embedding of the specimens (Morio et al. 1993). Adjusting exactly the incidence angle of the electron beam to the zone axis of the crystal for HREM is necessary. Therefore, technical improvements, such as an exact adjustment of the incidence angle of the electron beam in future observations of HREM images, in addition to improving the procedures of the specimens, should be done.

Some trematodes have crystalline inclusions in the neodermal cytoplasm. The neodermis of *Schistosoma mekongi* has three types of neodermal inclusions: discoid and membraneous bodies and spherical vesicles (Sobhon et al. 1984). The neodermis of adult *Schistosoma mansoni* has two characteristic inclusions: elongated and membraneous bodies (Hockley 1973). Electron microscopy of inclusions in *Paragonimus westermani* has shown inclusions that have linear, dotted, or homogeneous patterns depending on the plane of the sections (Fukuda et al. 1982). *Clonorchis sinensis* and *Opisthorchis viverrini* have crystalline inclusions that are minute circular granules in subtegumental cells (Inatomi et al. 1968, 1971). These various types of inclusions are clearly different from the cubic crystal protein inclusions in the neodermis of pancreatic flukes.

Among crystalline proteins in trematodes, glutathione S-transferase (GST) has been collected from *Schistosoma japonicum* (Lim et al. 1994), *Schistosoma haematobium* (Johnson et al. 2003), *C. sinensis* (Han et al. 2001), and *Fasciola hepatica* (Rossjohn et al. 1997). These studies described the crystal structure and crystallization of the cytosol of neodermal cells of flukes. A monoclonal antibody against recombinant GST of *Fasciola gigantica* showed a cross-reaction with *S. mansoni* and *S. japonicum* antigens, but no cross-reaction was detected with antigens of *Eurytrema* (Khawsuk et al. 2002). By using the antiserum of recombinant GST of *O. viverrini*, no or only a weak cross-reaction was observed against GST of some flukes, including *Eurytrema* (Eursitthichai et al. 2004). Accordingly, crystalliferous cytosolic proteins, such as GST, may be qualitatively different from cubic crystals protein inclusions in *Eurytrema*.

In this study, cubic crystal inclusions were histochemically stained with bromophenol blue, and the bands separated by using SDS-PAGE were stained with CBB. The stainability of the cubic crystal inclusions for the two dyes indicates that the crystal inclusions were composed of protein. The molecular weight of protein in the cubic crystal inclusions was 36.6 kDa by using SDS-PAGE. EDS showed a spike corresponding to sulfur. From these findings, the protein in cubic crystal inclusions may contain sulfur-containing amino acids. GST also contains sulfur. Therefore, an obvious great need is for future investigations into the more detailed biochemical structure and functional importance of the protein in cubic crystal bodies.

Acknowledgments This research was supported by the grant-in Aid for Scientific Research Program of Ministry of Education, Scientific and Culture of Japan (no. 58860045). The experiments comply with the current law of the countries in which the experiments were done.

References

- Chinone S, Fukase T, Itagaki H (1984) Experimental infection of domestic cats with *Eurytrema pancreaticum* and *E. coelomaticum* (Trematoda, Dicrocoeliidae). *Jpn J Parasitol* 33:29–39
- Eursitthichai V, Viyanant V, Vichasri-Grams S, Sobhon P, Tesana S, Upatham SE, Hofmann A, Korge G, Grams R (2004) Molecular cloning characterization of a glutathione S-transferase encoding gene from *Opisthorchis viverrini*. *Asian Pac J Allergy Immunol* 22:219–228
- Fukuda K, Fujino T, Hamajima F (1982) Crystalline inclusions in the subtegumental cells of the adult lung fluke, *Paragonimus westermani*. *Z Parasitenkd* 68:235–238
- Han YH, Chung YH, Kim TY, Hong SJ, Choi DJ, Ghung YJ (2001) Crystallization of *Clonorchis sinensis* 26 kDa glutathione S-transferase and its fusion protein with peptides of different lengths. *Acta Crystallogr D Biol Crystallogr* 57:579–581
- Hockley DJ (1973) Ultrastructure of the tegument of *Schistosoma*. *Adv Parasitol* 11:233–305
- Ilha MR, Loretto AP, Reis AC (2005) Wasting and mortality in beef cattle parasitized by *Eurytrema coelomaticum* in the state of Parana, south Brazil. *Vet Parasitol* 133:49–60
- Inatomi S, Tongu Y, Sakumoto D, Itano K, Suguri S (1968) The ultrastructure of helminth. I. The body wall of *Clonorchis sinensis* (Cobbold 1875) Looss, 1907. *Jpn J Parasitol* 17:395–401
- Inatomi S, Tongu Y, Sakumoto D, Suguri S, Itano K (1971) The ultrastructure of helminth. VI. The body wall of *Opisthorchis viverrini* (Poirier, 1886). *Acta Med Okayama* 25:129–142
- Johnson KA, Angelucci F, Bellelli A, Herve M, Fontaine J, Tsemoglou D, Capron A, Trottein F, Brunori M (2003) Crystal structure of the 28 kDa glutathione S-transferase from *Schistosoma haematobium*. *Biochemistry* 42:10084–10094
- Khawsuk W, Soonklang N, Grams R, Vichasri-Grams S, Wanichanon C, Meepong A, Chaithirayanon K, Ardseungneon P, Viyanant V, Upatham SE, Sobhon P (2002) Production and characterization of a monoclonal antibody against recombinant glutathione S-transferase (GST) of *Fasciola gigantica*. *Asian Pac J Allergy Immunol* 20:257–266
- Laemmli UK (1970) Cleavage of structural proteins during the assembly of the head of bacteriophage T4. *Nature* 227:680–685
- Lim K, Ho JK, Keeling K, Gilliland GL, Ji X, Ruker F, Carter DC (1994) Three-dimensional structure of *Schistosoma japonicum* glutathione S-transferase fused with a six-amino acid conserved neutralizing epitope of gp41 from HIV. *Protein Sci* 3:2233–2244
- Mazia D, Brewer PA, Alfert M (1953) The cytochemical staining and measurement of protein with mercuric bromophenol blue. *Biol Bull* 104:57–67
- Morio S, Baba N, Takabayashi K, Oh H, Yoshida S, Nagano T (1993) The crystal structure of specific granules in human eosinophils studies by thin sectioning and deep-etching with the aid of Fourier transformation. *J Electron Microsc* 42:172–177
- Moriyama N (1982) Karyological studies of bovine pancreatic flukes (*Eurytrema* sp.) and their phenotypes. *J Parasitol* 68:898–904
- Rossjohn J, Feil SC, Wilce MC, Sexton JL, Spithill TW, Parker MW (1997) Crystallization, structural determination and analysis of a novel parasite vaccine candidate: *Fasciola hepatica* glutathione S-transferase. *J Mol Biol* 273:857–872
- Sakamoto T, Kono I, Yasuda N, Yamaguti C (1980) Studies on *Eurytrema coelomaticum* I. Preliminary observations on the biological characters of *E. coelomaticum*. *Mem Fac Agric Kagoshima Univ* 16:83–92

- Sakamoto T, Tanimura I, Seki I (1985) Study of *Eurytrema coelomaticum* V. Electron microscopical observations on the tegument and associated structures of adult *Eurytrema coelomaticum*. J Fac Agric Iwate Univ 17:307–319
- Sobhon P, Upatham ES, McLaren DJ (1984) Topography and ultrastructure of the tegument of adult *Schistosoma mekongi*. Parasitology 89:511–521
- Tang Z, Tang C (1977) The biology and epidemiology of *Eurytrema coelomaticum* (Giard et Dillet, 1892) and *Eurytrema pancreaticum* (Janson 1889) in cattle and sheep in China. Acta Zool Sin 23:267–282
- Yamaguti S (1958) Systema helminthum. 1. Interscience, New York
- Yamaguti S (1971) Synopsis of digenetic trematodes of vertebrates. 1. Keigaku, Tokyo, Japan